

# Performance evaluation of a photovoltaic park in Cyprus using irradiance sensors

Rogiros Dimitris Tapakis, Alexandros George Charalambides\*

*Cyprus University of Technology, Department of Environmental Science and Technology  
Corner of Athinon and Anexartisias, 57, 3603, Lemesos, Cyprus*

## Abstract

The power output of Photovoltaic (PV) modules is directly affected by the presence of clouds, due to changes in the irradiance caused by clouds, resulting in rapid fluctuations of the solar electricity generation of PV Parks. Thus, the computation of the performance of PV parks under cloudy conditions is essential for the optimal operation of the electricity grid. This paper presents solar irradiance measurements to be used to simulate the performance of a grid connected PV park, based on the incident global irradiance at the photovoltaic modules. The 150kW<sub>p</sub> PV Park is located on an inclined roof of an industrial building in Limassol Cyprus (latitude 34.7°N, longitude 32.94°E). The incident irradiance at the PV modules is computed as the sum of three components: the beam component from direct irradiation of the tilted surface, the diffuse component, and the reflected component. The measurements of the diffuse and global horizontal irradiance were recorded on site using a BF-5 Sunshine Sensor and the tilted irradiance using the Sunny SensorBox. The measurements from the BF-5 Sunshine Sensor were previously validated against measurements from our meteorological station. For the computation of tilted irradiance, three isotropic and seven anisotropic models were used, using only measurements of global irradiance and calculations of solar position and irradiance incidence angle on the PV panels. The solar electricity generation of the park was correlated to the irradiance measurements from the Sunny SensorBox, taking into consideration the interconnection of the Park and the measurements of the module temperature provided by a monitoring system located on-site. The power output of the PV modules to the inverters for different incident irradiance was estimated from the current-volt characteristic curves of the PV modules based on the assumption that the inverters' maximum power point tracking mechanism adapts instantly to the fluctuations of solar irradiance, and thus, the PV modules always operate at maximum power output conditions. The influence of temperature on the power output of the PV modules was also introduced using the temperature coefficients of the PV modules. Results showed good agreement between measured and calculated power output.

**Keywords:** Solar Electricity Generation, Global Tilted irradiance, Photovoltaics, Simulation

## 1. Introduction

Despite the major progress made in the use of solar energy during the past years, and the large scale installations built, mainly Photovoltaics (PVs) and to

\*Corresponding author

*Email addresses:* rd.tapakis@edu.cut.ac.cy  
(Rogiros Dimitris Tapakis), a.charalambides@cut.ac.cy  
(Alexandros George Charalambides\*)

a lesser extent of Solar Thermal Power Plants, Solar Renewable Energy Systems (RES) have not yet achieved high penetration in the energy sector compared to the existing fossil fuel power plants. This is mainly due to their dependency on the variability of the sun's irradiance and in most cases, due to the lack of affordable storage options which leads to the attenuation of the power output of the solar RES. This dependency is more profound during partial cloudy conditions, when the fluctuations of solar irradiance over the solar field of the PV Park, due to the presence of the clouds in front of the sun disk result in the attenuation of the power output of the system.

However, since the instantaneous demand for electricity remains the same, a disparity arises between electricity production and demand that puts the stability of the grid at risk preventing the Transmission System Operator (TSO) from relying on solar RES for electricity generation. Providentially, base-load power plants are able to accommodate this instability by adjusting the electricity production from fossil fuel turbines; however, it is impossible to control the stability of the grid continuously during the day, due to the slow response of the traditional steam turbines. The most common solution, especially during daylight hours, is the production of electricity from the base-load power plants at levels above what is necessary, in order to regulate the fluctuations in electricity production from RES.

Aiming to eliminate unnecessary energy loss, an alternative solution launched recently is the short-term forecast horizons of the Solar Electricity Generation (SEG) of the solar RES, ranging from 1/2 hour to four hours and mid-term forecast horizons ranging from four to 24 hours. In order to achieve this, transnational electricity markets at first, followed by national electricity markets, give electricity producers a variable feed-in tariff option [1, 2]. This option motivates the operators of power plants to optimize the plant's performance over maximum profit by predicting the electricity production of their plant for a specified time horizon. In Italy for example, the feed-in-law motivates photovoltaic production with 20% extra revenue for accurate hourly prediction of the expected solar electricity production for the next day if the mean daily error is less than 10% for 300 days in one year [3].

The SEG of PV parks can be forecasted using three different methods [4]. The first is based on statistical or artificial intelligence techniques that are used to forecast directly the SEG of the PV Park based on the variation of the performance of the system over time, usually using supervised techniques [5]. The second method is the physical approach, which is based on predicting incident solar irradiance at the PV plane and the corresponding power output of the system taking into consideration the characteristics of the PV Park, the interconnections of the PV modules to the inverters, the shading of the modules and the Module Temperature ( $T_{mod}$ ) [6]. In this case the knowledge of incident solar irradiance is essential for the forecasting of SEG. The third method is a combined or hybrid approach of the physical models and the artificial intelligence techniques [1].

There are numerous models for the computation of solar radiation, ranging from complicated computer algorithms to very simple empirical relations that do not require any meteorological parameter as input. From these parameters, the most profound parameter for solar irradiance variations is cloudiness, because, although it can be predicted, the spatial and temporal resolution of the predictions is very low, resulting to an uncertainty in solar energy generation prediction. The other parameters can be computed using existing numerical forecasting methods [7]. The presence of clouds over the solar field of a PV park results in an increase of diffuse irradiance, which, depending on the obscuring of the sun, leads to a decrease of Direct Normal Irradiance (DNI) on the PV plane; incident global irradiance is thus respectively influenced. Consequently, the state of the sky defines the global, direct and diffuse irradiance on the solar field of the PV Park. In general, the prediction of solar irradiance is computed either directly, or by estimating the state of the sky over the PV park by computing the cloud motion vectors [8, 9] followed by the computation of incident irradiance on the PV plane.

The aim of our research is to compute the incident irradiance on the tilted PV plane based on irradiance measurements and simulate the performance of a PV park under variable irradiance conditions. The only inputs to the model are the Surface Air Temperature ( $T_{sur}$ ) and irradiance measurements consisting only

of global and diffuse horizontal irradiance measurements on the horizontal plane. These three parameters were selected since Global Horizontal Irradiance (GHI) and diffuse irradiance are easily computed if the state of the sky is known [10–12] while  $T_{sur}$  is correlated to the Cloud Cover (CC) and solar irradiance [13, 14] and the  $T_{sur}$  can be modelled by defining the normalized CC- $T_{sur}$  relationship [15].

## 2. Equipment and computational Model

The measurements for the computations were obtained on-site from a grid connected PV Park of 150 kW<sub>p</sub> installed capacity, installed on an inclined roof of an industrial building in Limassol Cyprus (34.73°N, 32.94°E). The PV Park consists of 652 modules type 60E6M+230F(L) manufactured by Enfoton Solar LTD and 9 inverters type STP 17000TL manufactured by SMA. The efficiency of the panels is 17.1% while the Max and Euro-ETA efficiency of the inverters are 98.1% and 97.7% respectively.

Each inverter has 2 MPP trackers where a different number of PV modules can be connected in series. Five of the inverters have 18 modules per string (4×18) while the other four have 18 modules per string in the first MPP and 19 in the second (3×18, 1×19).

The plant was installed during July 2012 and covers approximately 1040 m<sup>2</sup>. The slope tilt of the roof is 20° and the azimuth is -23°. The annual yield of the PV Park for 2013 was 273.39 MWh, which corresponds to 1784.8 kWh/kWp.

The PV Park has a meteorological station based on the SMA Sunny SensorBox that measures global irradiance at the PV plane (i.e. tilted), ambient and module temperature and air speed. The maximum, minimum and average values of the meteorological data of the PV park are recorded every 15 minutes while the corresponding measurements of the current (I), volt (V) and power (P) inputs from each string, and the SEG of each inverter are recorded every hour. All the measurements are stored and can be accessed via an internet connection for further computations through the SMA WebBox.

Fig. 1 presents the location of the PV park, demonstrating the orientation of the PV modules and mea-

suring sensors and control room.

Solar irradiance was measured using the BF-5 Sunshine Sensor manufactured by Delta-T Devices [16] which was installed next to the tilted global irradiance sensor on the roof of the building. BF-5 is a remote sensor that measures GHI and diffuse irradiance simultaneously. BF-5 measurements were recorded every 10 seconds and were stored on the computer for further computations.

In order to verify the accuracy of the BF-5 Sunshine Sensor, the irradiance data from the instrument were previously validated against the measurements of GHI and diffuse irradiance from a meteorological station positioned on the roof-top of the university building in Limassol Cyprus (34.68°N, 33.05°E). The meteorological station is a remote station based on Geónica's Meteodata 3000 data transmission system that records the one-minute maximum, minimum and average values of GHI, DNI, diffuse irradiance, wind speed and direction, humidity and ambient temperature. The pyranometers of the station (for GHI and diffuse irradiance) are ISO 9060 Secondary Standard pyranometers model MS-802, manufactured by EKO, with a response time of 5 seconds [17].

Table 1 presents the monitor parameters of the sensors that were used for this research, the units of each parameter and the time period for each measurement. All recorded values composed of the average, minimum and maximum value for the specific time period.

The measurements for the validation were recorded in the period December 2012 to February 2013. At first, the one-minute maximum and average values of the measurements from the BF-5 sensor were computed and then they were compared to the measurements of the meteorological station.

Fig. 2 presents the comparison of the measured GHI (Fig 2a) and diffuse irradiance (Fig 2b) as acquired by the BF-5 sensor and corresponding measurements from the meteorological station for the two months period. As can be seen on the Fig. from  $R^2$  and the slope of the best-fit line, the measurements of both global and diffuse irradiance of the BF5 approximate the measurements from the meteorological station.

The RMSE and MBE for GHI were 80.65 W/m<sup>2</sup>

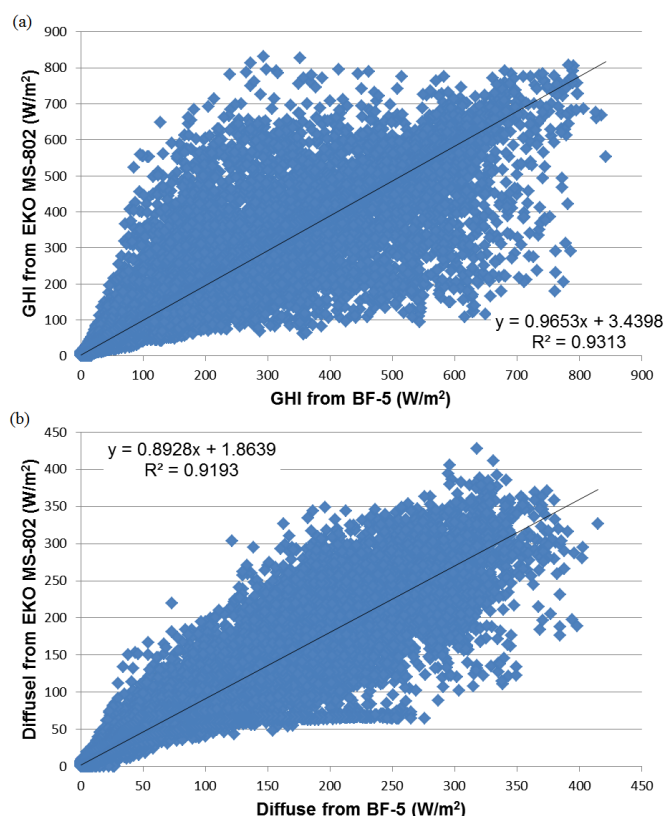


Figure 2: Comparison of (a) GHI and (b) diffuse irradiance measurements from the BF-5 towards the measurements from the EKO MS-802 pyranometers

and  $0.64 \text{ W/m}^2$  respectively whereas for the diffuse were  $37.59 \text{ W/m}^2$  and  $10.49 \text{ W/m}^2$  respectively.

From the validation of the data it was observed that most discrepancies were recorded during the early morning and late afternoon hours, where the sun is at low elevation angles and diffuse irradiance is higher. Thus, the comparison was computed again only for the measurements recorded from 09:00 to 15:00 (local time) and is presented in Fig. 3.

Fig. 3 presents the comparison of the measured GHI (Fig 3a) and diffuse irradiance (Fig 3b) as acquired by the BF-5 sensor and the corresponding measurements from the meteorological station for the selected daylight hours (09:00...15:00 local hour). As can be seen from  $R^2$  and slope of the best-fit line in the Figs, the results of the comparison have improved, especially for the diffuse irradiance. It is now evident that any "errors" in the measurements are in the early morning and late afternoon time, thus, not significant for the forecasting of the power out-

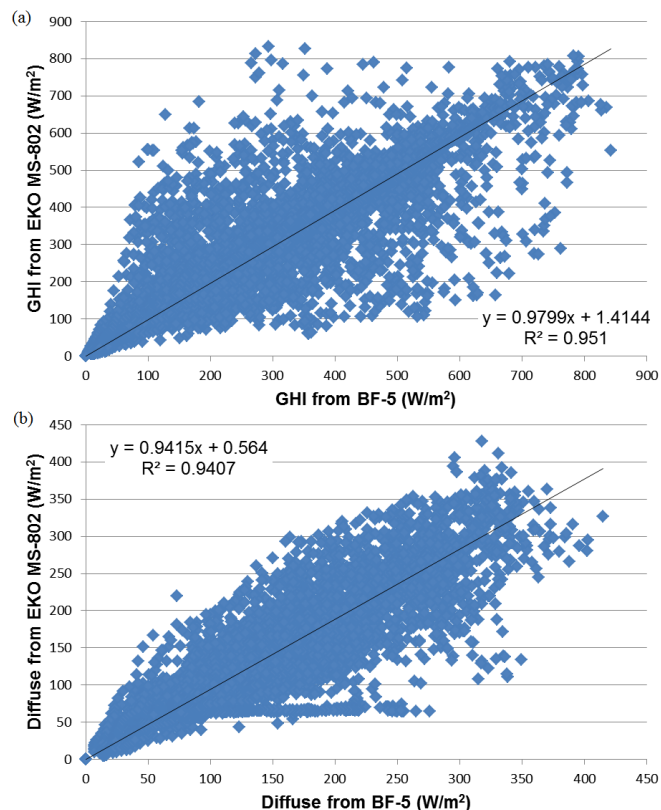


Figure 3: Comparison of (a) GHI and (b) diffuse irradiance measurements from the BF-5 towards the measurements from the EKO MS-802 pyranometers for hours 09:00...15:00

put of PV parks. The RMSE and MBE for GHI were  $81.3 \text{ W/m}^2$  and  $-3.2 \text{ W/m}^2$  respectively whereas for the diffuse were  $35.5 \text{ W/m}^2$  and  $4.3 \text{ W/m}^2$  respectively.

### 3. Computation of Global Tilted Irradiance

Although the necessity of using global tilted irradiance is acknowledged for the computations of the performance of PV Parks, most meteorological stations only have measurements of GHI and in most cases, diffuse irradiance. Thus, various models were proposed for the computations of global tilted irradiance at any tilt angle and azimuth [18–20]. These models are primarily to accommodate the peculiarities in solar irradiance requirements for each solar energy application, depending on the angle of the solar collector, the azimuth and the tracking possibilities of each application. Thus, irradiance values at the horizontal are recorded by the meteorological stations and then, depending on the characteristics of

the solar application, the incident irradiance is computed. In the case of fixed angle PV Parks, the incident irradiance is represented by the global tilted irradiance.

Fig. 4 presents the measurement of GHI (blue line) and diffuse irradiance (red line) for six different days from February to June 2013 during cloudy and clear sky conditions using the BF-5 sensor. As was expected, during cloudy conditions, the profile of the fluctuations of the diffuse irradiance corresponds to the profile of the fluctuations of the GHI, while during cloudy free conditions the profile is roughly constant, thus, indicating the proper functioning of the sensor.

In general, global tilted irradiance is computed as the sum of three components: beam component of direct irradiation on the tilted surface, diffuse tilted and reflected irradiance. Beam tilted is computed from GHI, diffuse irradiance and incident angle of the irradiance on the tilted surface. Diffuse tilted is computed by multiplying the diffuse irradiance with the diffuse transposition factor ( $R_d$ ) which represents the ratio of diffuse radiation on a tilted surface to that of a horizontal surface, using simple or more complex models. Simpler models assume that the diffuse irradiance is isotropic and exhibits a uniform distribution over the sky dome, while Circumsolar and horizon brightening parts are assumed to be zero. In these models, the only input parameter is the surface tilt angle with respect to the horizontal plane. More complex models take into consideration the anisotropic behavior of diffuse irradiance introducing inherent anisotropic factors such as circumsolar radiation, sky conditions and horizon brightening. Finally, the reflected component of irradiance can be assumed as isotropic and is dependent on GHI, albedo and tilt angle [18–20].

Overall, ten models were used to compute global tilted irradiance and were evaluated towards future on-site measurements. Three models are isotropic models, viz. Liu Jordan model, Korokanis model, and Badescu model, while seven are anisotropic, viz. Willmot model, Bugler model, Ma-Iqbal model, Hay model, Skartveit-Olseth model, Reindel model and Temps-Coulson model. a detailed description of the equations of the models is presented by Demain et al. [18].

The measurements used for the computations were recorded during February and March 2013. The input data to the computations were the GHI and diffuse irradiance recorded from the BF-5 and the measurements of the tilted global irradiance recorded by the Sunny SensorBox. Since the measurements from the BF-5 were recorded every 10 seconds, the 15-minute minimum values of the tilted irradiance for each model were computed and used for the comparison.

Table 2: Statistical analysis of the performance of the ten models from the comparison of computed and measured minimum values of Global Tilted Irradiance for the period February...March 2013

	Model	RMSE, W/m <sup>2</sup>	MBE, W/m <sup>2</sup>
1	Liu Jordan	148.0	44.6
2	Korokanis	147.4	44.0
3	Badescu	149.5	46.3
4	Willmot	214.0	48.6
5	Bugler	6468.0	296.2
6	Ma-Iqbal	146.0	41.0
7	Hay	147.6	43.2
8	Skartveit-Olseth	148.0	43.6
9	Reindel	147.6	43.1
10	Temps-Coulson	137.0	19.9

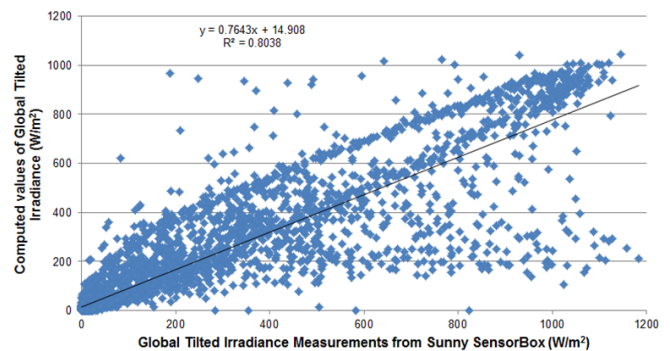


Figure 5: Comparison of computed and measured minimum values of Global Tilted Irradiance for the period February...March 2013

The statistical results of the comparison of the computed and measured minimum values of global

tilted irradiance for the ten models are presented in Table 2. As can be seen, the results from the Temps-Coulson model showed the highest accuracy; RMSE and MBE were  $137.0 \text{ W/m}^2$  and  $29.9 \text{ W/m}^2$  respectively. Fig. 5 presents the comparison of the measured global tilted irradiance as acquired by the Sunny SensorBox and the corresponding computations of the Temps-Coulson model using the measurements from the BF-5 for the period February...March 2013.

#### 4. Simulation of Performance of PV modules

The simulation of the performance of the PV Park was developed based on a supervised algorithm that computes the  $P$ ,  $I$  and  $V$  output of the PV modules for varying incident irradiance and  $T_{mod}$  conditions and then the corresponding power output from the PV inverters. At first, the values of  $I$ ,  $V$  and  $P$  of the PV module are computed for incremental values of incident irradiance and  $T_{mod}$  based on the temperature coefficients provided by the manufacturer and the components database of PVSYST [21]. The values of incident irradiance and  $T_{mod}$  ranged from  $10 \text{ W/m}^2$  to  $1,300 \text{ W/m}^2$  and  $10^\circ\text{C}$  to  $75^\circ\text{C}$  respectively. Then, based on the computed values, the correlation for each parameter ( $I$ ,  $V$  and  $P$ ) is modelled using cubic splines interpolation and each parameter is computed for different pairs of incident irradiance and  $T_{mod}$ .

Thus, the only inputs to the models are the incident irradiance and  $T_{mod}$ . Incident irradiance can be computed from the values of GHI and diffuse irradiance from the BF-5 sensor, using the methodology presented in Section 3. On the other hand,  $T_{mod}$  varies for different weather conditions and has to be modelled first. Skoplaki et al. [22] proposed simplified correlations for the computation of  $T_{mod}$  depending to the ambient temperature, the solar irradiance and Nominal Operating Cell Temperature (NOCT); the value of NOCT is specified by the manufacturer of the PV module. Correspondingly, Tofighi [23] presented a dynamic thermal model of the PV module where the module operating temperature was modelled using three parameters as input: solar irradiance, ambient temperature and wind speed.

Additionally, the free stream wind speed (as a relation of the local wind speed) may be integrated to the correlations to improve the accuracy of the computations. Hence, the  $T_{mod}$  can be modelled for the specific PV module in relation to the incident irradiance and ambient temperature.

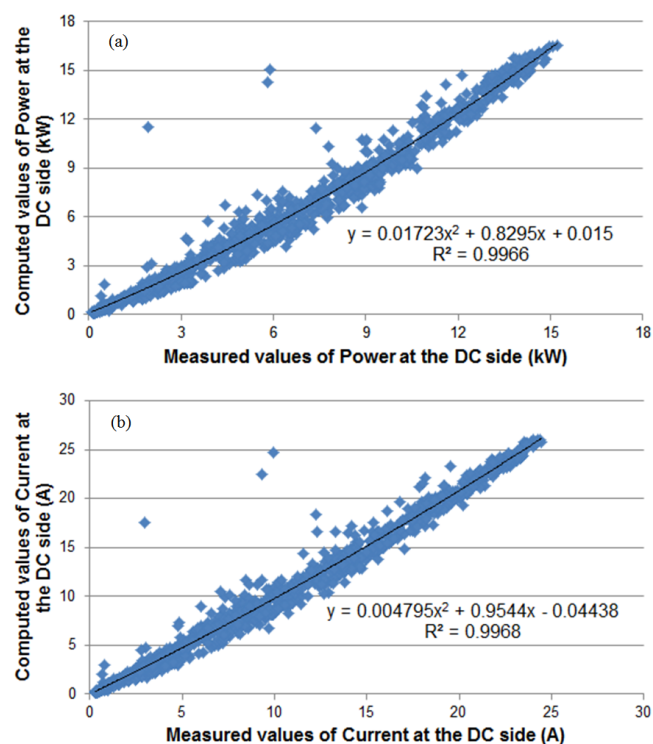


Figure 6: Comparison of hourly values of (a) Power and (b) Current computations at the DC site of the inverter towards the corresponding measurements as recorded from the inverter for the period January...June 2013

The hourly values of Power and Current at the DC side of the inverter were computed based on the Incident Irradiance and  $T_{mod}$  measurements from the Sunny SensorBox using the developed simulation model. Consequently, the computed values were compared to the corresponding hourly values of Power and Current, recorded by one of the inverters of the PV Park. Fig. 6 presents the comparison of the computed towards the measured values of the Power (Fig 6a) and Current (Fig 6b) at the DC side of the inverter for the period January to June 2013. The RMSE and MBE for the Power were  $0.79 \text{ kW}$  and  $-0.13 \text{ kW}$  respectively, whereas for the Current were  $1.08 \text{ A}$  and  $0.05 \text{ A}$  respectively. The best fit correlation curve for each parameter and the corresponding equations are also presented in the Fig..

Subsequently, the power output of the inverters can be computed in relation to the input  $P$  from the PV modules and the efficiency of the inverter. Since the efficiency of the inverter is variable, it has to be first modelled. Inverter's efficiency is specified by the manufacturer by the efficiency curves, dependent to the DC Voltage input and the rated power from the PV modules. Thus, the number of PV modules per string defines both the  $V$  and  $P$  inputs to the inverter. Therefore, based on the characteristic curve of the inverters and the number of PV modules per string for the different interconnections of modules to the inverters, the power output of each inverter can be modelled.

## 5. Conclusions

This paper presents the methodology for the development of a computational model of the performance of a PV Park under variable irradiance conditions. The proposed methodology can be used for forecasting the SEG of the PV Parks under cloudy conditions given the state of the sky. The computational algorithms for the individual parts of the proposed methodology and the validation of the BF5 instrument against a high precision meteorological station are presented.

Incident irradiance was computed in relation to the GHI and diffuse irradiance based using ten computational models. Additionally, the performance of a 150 kW<sub>p</sub> PV Park installed at a rooftop of an industrial building in Cyprus was simulated based on the incident irradiance on the PV modules and the module temperature.

Good agreement was shown from the comparison of the computed towards the measured values. The measurements of global and diffuse irradiance of the BF5 approximated the measurements from the meteorological station; the RMSE and MBE for GHI were 81.3 W/m<sup>2</sup> and -3.2 W/m<sup>2</sup> respectively whereas for the diffuse were 35.5 W/m<sup>2</sup> and 4.3 W/m<sup>2</sup> respectively. The best fit model for the computation of incident irradiance was the Temps-Coulson model; RMSE and MBE were 137.0 W/m<sup>2</sup> and 29.9 W/m<sup>2</sup> respectively. Finally, very accurate correlation was achieved for the simulation of the PV system between the measured parameters and the computa-

tional results. The RMSE and MBE for the Power at the DC side were 0.79 kW and -0.13 kW respectively, whereas for the Current were 1.08 A and 0.05 A respectively.

In future work, better temporal resolution data will be used as inputs to the calculations in order to extract more accurate results and data from an all-sky camera will be incorporated to the model in order to develop an integrated simulation model that will compute the SEG of the PV Park based only on the state of the sky over the solar field of the PV Park.

## Acknowledgments

The authors would like to thank Johnsun Heaters LTD and Allison Fashion LTD for providing the facilities and software to conduct this research.

## References

- [1] L. A. Fernandez-Jimenez, A. Munoz-Jimenez, A. Falces, M. Mendoza-Villena, E. Garcia-Garrido, P. M. Lara-Santillan, E. Zorzano-Alba, P. J. Zorzano-Santamaria, Short-term power forecasting system for photovoltaic plants, *Renewable Energy* 44 (2012) 311–317.
- [2] P. Bacher, H. Madsen, H. A. Nielsen, Online short-term solar power forecasting, *Solar Energy* 83 (2009) 1772–1783.
- [3] A. Bracale, P. Caramia, U. De Martinis, A. R. Di Fazio, An improved bayesian-based approach for short term photovoltaic power forecasting in smart grids, in: *Proc. International Conference on Renewable Energies and Power Quality (ICREPPQ'12)*, Santiago de Compostela, Spain, 2012.
- [4] E. Lorenz, D. Heinemann, *Comprehensive Renewable Energy*, Elsevier LTD, 2012, Ch. Prediction of Solar Irradiance and Photovoltaic Power, pp. 239–292.
- [5] A. Mellit, S. Saglam, S. A. Kalogirou, Artificial neural network-based model for estimating the produced power of a photovoltaic module, *Renewable Energy* 60 (2013) 71–78.
- [6] K. H. Lam, W. C. Loc, W. M. Tob, The application of dynamic modelling techniques to the grid-connected pv (photovoltaic) systems, *Energy* 46 (2012) 264–274.
- [7] R. Tapakis, A. G. Charalambides, Equipment and methodologies for cloud detection and classification: A review, *Solar Energy* 92 (2012) 392–430.
- [8] H. Escrig, F. J. Batlles, J. Alonso, B. F. M., B. J. L., I. B. Salbidegoitia, B. J. I., Cloud detection, classification and motion estimation using geostationary satellite imagery for cloud cover forecast, *Energy* 55 (2013) 853–859.
- [9] C. W. Chow, B. Urquhart, M. Lavea, A. Domingueza, J. Kleissl, J. Shields, B. Washom, Intra-hour forecasting with a total sky imager at the uc san diego solar energy testbed, *Solar Energy* 85 (2011) 2885–2893.

- [10] M. A. Mosalam Shaltout, A. H. Hassen, Solar energy distribution over egypt using cloudiness from meteosat photos, *Solar Energy* 45 (1990) 345–351.
- [11] Y. Dazhi, P. Jirutitijaroen, W. M. Walsh, Hourly solar irradiance time series forecasting using cloud cover index, *Solar Energy* 86 (2012) 3531–3543.
- [12] V. Badescu, A new kind of cloudy sky model to compute instantaneous values of diffuse and global solar irradiance, *Theoretical and Applied Climatology* 72 (2002) 127–136.
- [13] A. D. Erykin, T. Sloan, A. W. Wolfendale, Clouds, solar irradiance and mean surface temperature over the last century, *Journal of Atmospheric and Solar-Terrestrial Physics* 72 (2010) 425–434.
- [14] A. Dai, K. E. Trenberth, T. R. Karl, Effects of clouds, soil moisture, precipitation, and water vapor on diurnal temperature range, *Journal of Climate* 12 (1999) 2451–2473.
- [15] B. Sun, P. Y. Groisman, R. S. Bradley, F. T. Keimig, Temporal changes in the observed relationship between cloud cover and surface air temperature, *Journal of Climate* 13 (2000) 4341–4357.
- [16] Delta-T Devices.  
URL <http://www.delta-t.co.uk/>
- [17] Geonica.  
URL <http://www.geonica.com/>
- [18] C. Demain, M. Journee, C. Bertrand, Evaluation of different models to estimate the global solar radiation on inclined surfaces, *Renewable Energy* 50 (2013) 710–721.
- [19] A. Padovan, D. Del Col, Measurement and modeling of solar irradiance components on horizontal and tilted planes, *Solar Energy* 84 (2010) 2068–2084.
- [20] E. G. Evseev, A. I. Kudish, The assessment of different models to predict the global solar radiation on a surface tilted to the south, *Solar Energy* 83 (2009) 377–388.
- [21] PVSyst.  
URL <http://www.pvsyst.com/en/>
- [22] E. Skoplaki, A. G. Boudouvis, J. A. Palyvos, A simple correlation for the operating temperature of photovoltaic modules of arbitrary mounting, *Solar Energy Materials and Solar Cells* 92 (2008) 1393–1402.
- [23] A. Tofighi, Performance evaluation of pv module by dynamic thermal model, *Journal of Power Technologies* 93 (2) (2013) 111–121.

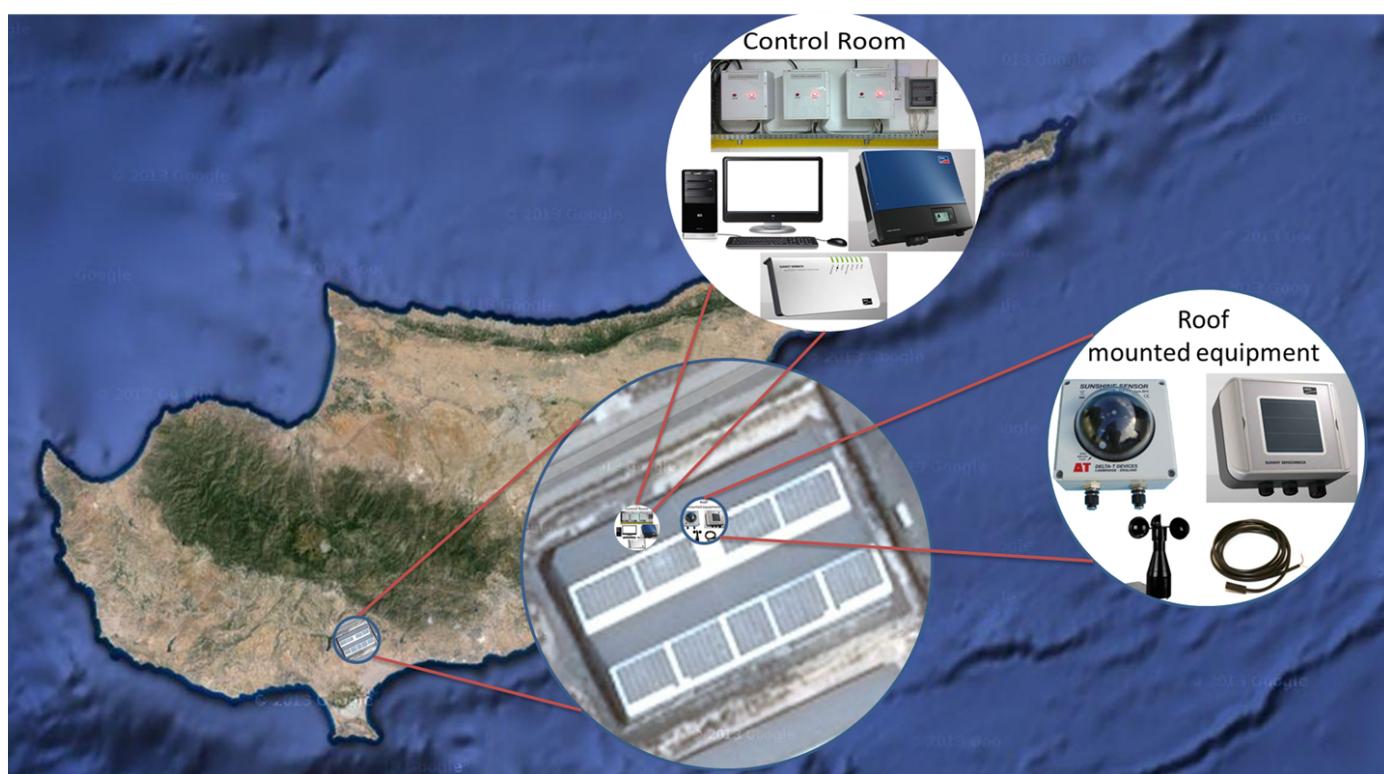


Figure 1: A schematic diagram of the PV park demonstrating the location of the PV park, the orientation of the PV modules, the location of the roof mounting equipment (irradiance, temperature and wind sensors) and the control room where the inverters, router and computer server are located

Table 1: Monitor parameters of the sensors that were used for this research

Instrument	Measuring Parameters	Time Period	Accuracy	Range
BF5	GFI, $W/m^2$	10 sec	$\pm 5 W/m^2$	0...1250
	Diffuse, $W/m^2$	10 sec	$\pm 20 W/m^2$	0...1250
SMA Sensor Box (via WebBox)	Incident Irradiance, $W/m^2$	15 min	$\pm 8\%$	0...1500
	$T_{mod}$ , $^{\circ}C$	15 min	$\pm 0.5^{\circ}C$	-20...110
	Ambient Temp, $^{\circ}C$	15 min	$\pm 0.5^{\circ}C$	-30...80
	Wind Speed, m/s	15 min	$\pm 0.5$ m/s	0.8...40
Inverter (via WebBox)	I, A	1 hour	$\pm 2\%$	–
	V, V	1 hour	$\pm 2\%$	–
	P, W	1 hour	$\pm 2\%$	–
	SEG, kWh	1 hour	$\pm 2\%$	–
EKO MS-802	GHI, $W/m^2$	1 min	$< 0.2 W/m^2$	0...2000
	Diffuse, $W/m^2$	1 min	$< 0.2 W/m^2$	0...2000

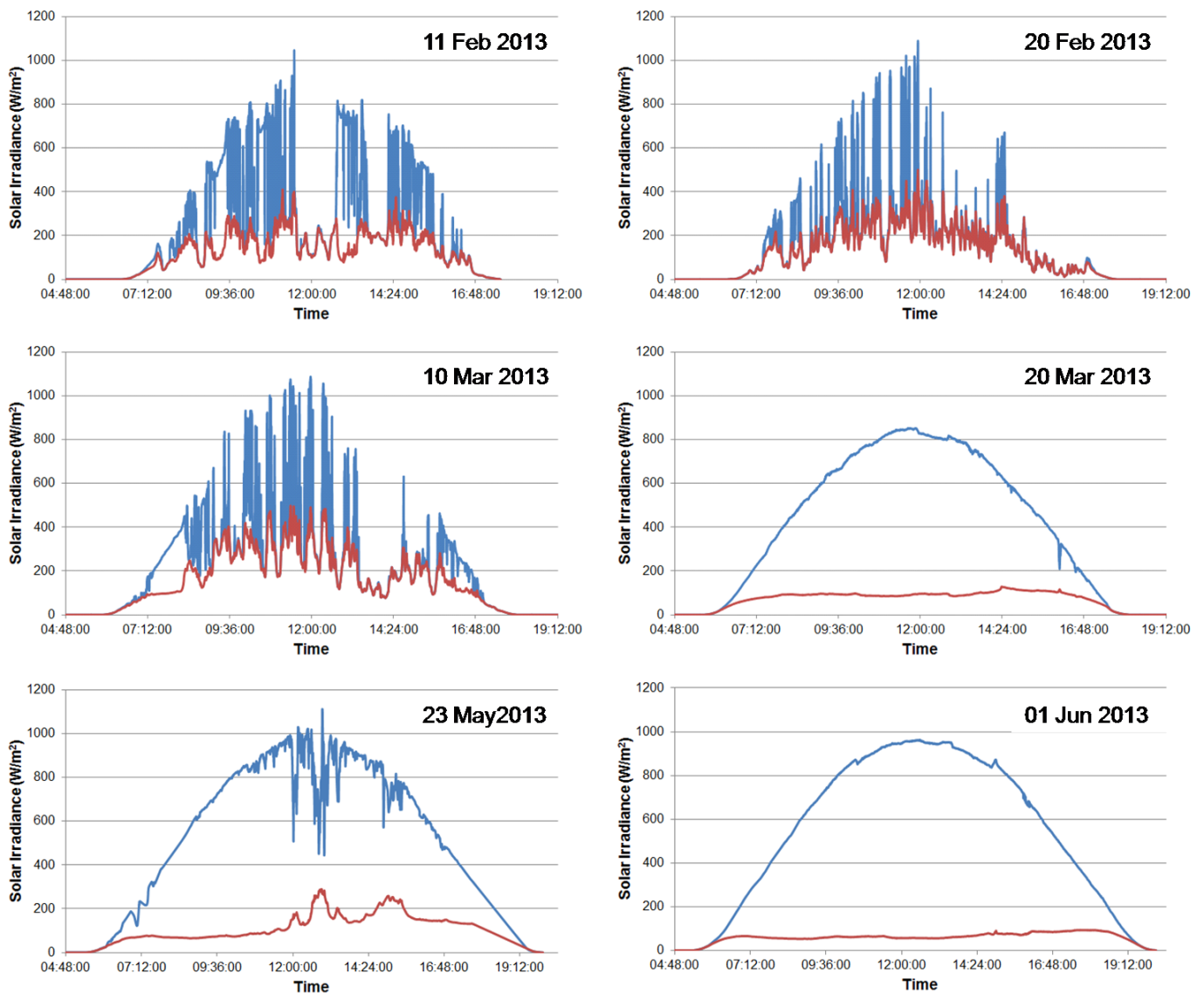


Figure 4: GHI (blue line) and diffuse irradiance (red line) measurements from BF-5 on site at the PV Park for six different days